PERGAMON

International Journal of Heat and Mass Transfer 45 (2002) 691–696

International Journal of HEAT and MASS TRANSFER

www.elsevier.com/locate/ijhmt

Technical Note

Visualization of boiling bubble dynamics using a flat uniformly heated transparent surface

C.C. Pascual [a], S.M. Jeter [b,*], S.I. Abdel-Khalik [b]

[a] *Mechanical Engineering Department, California Polytechnic State University, San Luis Obispo, CA 93407, USA*

[b] *George Woodruff School of Mechanical Engineering, Georgia Institute of Technology, Atlanta, GA 30332-0405, USA*

Received 1 June 2000; received in revised form 1 May 2001

Abstract

Bubble dynamics in saturated pool boiling of R-123 with and without an applied electric field have been investigated using a novel, flat, transparent heated surface. This method allows viewing and measurement of bubble dynamics from the entire heater surface without interference from the fluid or other bubbles. The data have been used to quantify the effect of an electric field on the latent heat contribution to the total heat flux and to demonstrate the effectiveness of this experimental technique. For a given heat flux, the application of the electric field reduces the surface temperature, thereby suppressing boiling and reducing the latent heat contribution.

1. Introduction

This investigation presents a novel technique for studying boiling bubble dynamics from flat rectangular surfaces. A transparent heater was used instead of a thin rectangular strip (see [1]), which allowed for easy imaging of the entire surface when the camera was placed beneath the surface. This imaging location also removed the effect of the fluid and/or interfering bubbles from the camera's field of view. Therefore, a direct measurement of detailed bubble dynamics over the entire surface and the corresponding contribution of various mechanisms to the total heat flux can be easily determined. Experiments have been performed with and without an applied electric field near the heated surface to demonstrate the effectiveness of the experimental technique and quantify the enhancement of boiling heat transfer on a flat surface with the application of a high voltage, low current, electric field. Application of an electric field to systems using dielectric coolants, e.g., R-123, is known to enhance heat transfer. This effect is commonly referred to as electrohydrodynamic (EHD) enhancement. The resulting increase in the heat transfer coefficient can reduce the size of a heat exchanger for a given load, and/or decrease the necessary temperature difference, thereby increasing thermal efficiency. In micro-gravity applications, the EHD force can be used to replace gravity, thereby allowing for effective use of pool boiling heat transfer.

2. Experimental apparatus

Saturated pool boiling of R-123 from an electrically heated flat surface was investigated. A schematic diagram of the experimental apparatus is shown in Fig. 1. A transparent flat heater made from indium tin oxide (ITO) was chosen to facilitate imaging of the boiling dynamics from beneath the heated surface. ITO is a thin film transparent electronic conductor that is simultaneously transparent to visible radiation and electrically conducting [2]. In contrast, metal films have difficulty simultaneously being both transparent and conductive. ITO, a semiconducting film, is made of indium oxide doped with 5–10 mol% of tin. Commercial grade ITO has a resistivity of approximately 2×10^{-4} Ω cm. Another property of ITO is that its

* Corresponding author. Tel.: +1-404-894-3211; fax: +1-404-894-8496.

E-mail address: sheldon.jeter@me.gatech.edu (S.M. Jeter).

0017-9310/02/$ - see front matter
PII: S0017-9310(01)00167-3

Nomenclature

$F(D)$	frequency distribution function defined such that $F(D)\,\mathrm{d}D$ is the number of bubbles per nucleation site leaving the heated surface per unit time with diameter between D and $D+\mathrm{d}D$ (s^{-1} m^{-1})	$\langle F\rangle$	average bubble departure frequency (s^{-1})
		$\langle J\rangle$	average heat removal per bubble (J)
		$\langle N\rangle$	average number of nucleation sites per area (cm^{-2})
		q''	latent heat flux ($\mathrm{W/cm}^2$)

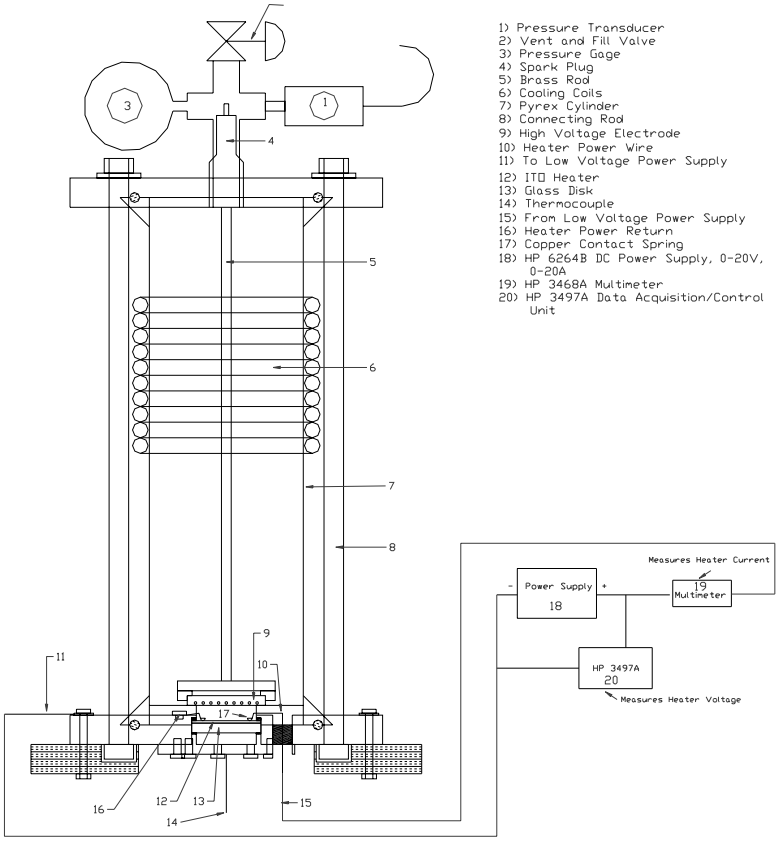

Fig. 1. Experimental test facility.

resistance change with temperature is linear. Therefore, by recording the resistance of the heater during experiments, the average surface temperature of the heater can be determined. To apply a uniform current density to the heater, i.e., to obtain a uniform heat flux over the entire surface, copper was plated to the edge of the ITO surface (see Fig. 2(a); refer to [3] for details about copper plating).

The final geometry for the heater was a 45 mm circular glass disk with a 0.30 μm layer of ITO. The actual heated portion of this circular disk was approximately a 15 mm long by 15 mm wide square, which resulted in a total resistance of approximately 7 Ω. To ensure that only this square region provided active nucleation sites, the ITO was removed from the surrounding glass. The ITO heaters used in the experiment ranged in size from 2.55 to 4.13 cm^2. A multimeter (HP3468A) was used to measure the current supplied to the surface (Fig. 1), while an external bus data acquisition system (HP3497A data acquisition/control unit) was used to measure the voltage drop across the surface. Based on the manufacturer's calibration, the multimeter was accurate to 0.14% of the reading for currents <1 A and 1% of the reading for currents >1 A. Also based on the manufacturer's calibration, the data acquisition system was accurate to 0.002% of the voltage reading. Even though the resistance of indium tin oxide changed linearly with temperature, the change was small. As a result, accurate

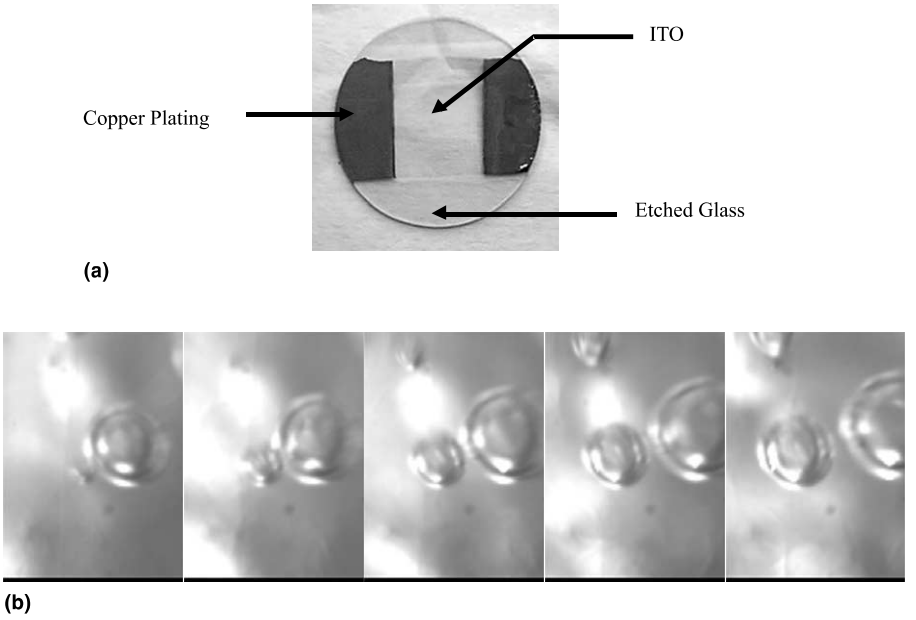

Fig. 2. (a) ITO heater. (b) Typical images from experiment at 5 W/cm^2.

surface temperature measurement requires highly accurate measurement of the resistance. Nevertheless, uncertainty in the surface temperature measurement may be significant, because the contact resistance between the electrode and copper spring contacts may change with applied power and mask the resistance change of the ITO. A 0–30 kV high voltage power supply supplied voltage to the electrode through the spark plug and brass rod (see Fig. 1). The ITO heater and the high voltage electrode were both submerged in the pool of liquid R-123, which was at saturation conditions. A complete description of the remainder of the experimental apparatus may be found in [4].

Bubble dynamics over the heated surface were imaged using a high speed digital camera (Dalsa CA-D1-128D) operated at 770 frames/s. Experiments were conducted at different power inputs (i.e., heat flux values) with and without an applied electric field. 100 images at approximately 100 locations along the surface were taken, i.e., a total of approximately 10,000 images were obtained for each of the 22 experiments conducted. These images were individually viewed to determine the average number of active nucleation sites, the bubble departure diameters, and the bubble departure frequencies. A more detailed description of the experimental procedure can be found in [3]. By imaging from underneath the heated surface, the effects of bubble interaction, interfering bubbles, and the liquid are eliminated. The camera can focus directly on the nucleation site and observe the bubble waiting period and the bubble growth period. This ability offers an advantage over traditional techniques, which measure the bubble dynamics from the side or above.

The three dominant sources of error in the experimental apparatus were the measured bubble diameter, the surface temperature, and the measured bubble departure frequency. To minimize the measured bubble diameter error, the largest magnification factor was used. Accurate surface temperatures were not achieved because of the varying contact resistance, which masked the resistance change of the ITO. The bubble departure frequency was fixed by the camera speed, which was at its maximum setting.

3. Experimental results

Bubble dynamics at five different heat flux values, viz., 5.0, 6.5, 8.0, 9.5, and 11.0 W/cm^2, with and without an applied electric potential up to 20 kV were examined. Fig. 2(b) shows typical bubble pictures recorded from below the ITO surface. In Fig. 2(b), a bubble is just beginning to grow near the center of the first picture; it continually grows and remains in focus, i.e., attached, as time progresses through the subsequent four frames.

The high speed video images were used to determine the effect of the applied electric field on the latent heat contribution to the total heat flux following the model of Paul and Abdel-Khalik [5]. The model subdivides the total heat flux for nucleate pool boiling into three parts: (1) latent heat transfer, (2) enhanced convection and

(3) natural convection. The latent heat transfer component corresponds to the energy removed from the heated surface due to phase change, while enhanced convection corresponds to the energy removed by forced convection resulting from fluid motion near the nucleation sites as the bubbles depart. Finally, the natural convection contribution corresponds to the energy removed from the surface regions unaffected by bubble dynamics.

The average surface heat flux was calculated from the measured heater current and voltage. The estimated average error in the heat flux was 2.2%; the major contributor to this bias error was the uncertainty in the measured heater area. The error propagation analysis was based on the method presented in [6]. The saturation temperature calculated from the measured system pressure matched the directly measured pool temperature, thus verifying saturation conditions inside the cylinder.

Each of the 22 sets of data consisted of approximately 10,000 images with 100 images at approximately 100 different positions, 1.87 mm wide by 2.59 mm tall in area, over the surface. At each of these 100 locations over the surface, all the nucleation sites were counted. The nucleation sites were identified by viewing all 100 images at each location in a movie format. The estimated error in the average number of nucleation sites per unit area, $\langle N \rangle$, was 5.0%; the largest source of precision error was the uncertainty in counting the number of active nucleation sites.

Owing to the large number of images for each experiment, a random sample of position locations was used to estimate the average bubble departure diameter. Therefore, approximately 14–83 random positions were chosen out of the total number of positions. At each of these random locations, the bubble departure diameters and the bubble departure frequencies were measured. To verify the validity of the random sample, bubble departure diameters and bubble departure frequencies were measured at each position in one experiment. Afterward, 20 locations were randomly chosen. The average bubble departure diameter and the average bubble departure frequency were compared between the complete analysis and the random sample. Based on statistical analysis, there was no statistically significant difference between the complete analysis and the random sample.

For each of the random locations, the bubble departure was identified by viewing a movie of the entire 100-image sequence. The corresponding bubble departure diameters were measured using a magnified printed image of the identified frame. Based on the measurement and magnification factor errors, the estimated bias error in the bubble diameter measurement was 0.04 mm. For a given heat flux, all the bubble data at the random locations were analyzed statistically. Figs. 3(a) and (b) show typical bubble departure diameter distributions. The dashed line is a normal distribution, while the solid line is the asymptotic expansion of the normal frequency function. While there was a slight skewness and kurtosis with most of the bubble departure diameter data, a normal distribution assumption introduced negligible error in the final analysis, and was, therefore, adopted. Fig. 3(a) shows results for a total heat flux of 5.11 W/cm^2 with no electric field, while Fig. 3(b) shows results for 5.02 W/cm^2 with an applied electric potential of 20 kV. The application of the electric field clearly resulted in a reduction in the average bubble departure diameter.

The average bubble departure frequency, $\langle F \rangle$, was determined from the experimental data, by counting the number of frames between consecutive bubble departures. The bubble period was calculated by dividing the number of frames by the frame rate (770 frames/s). At least 50 bubble departures were counted to obtain a statistically significant sample. The estimated bias error in the bubble departure period was 0.0013 s, which corresponded to the time between two consecutive frames.

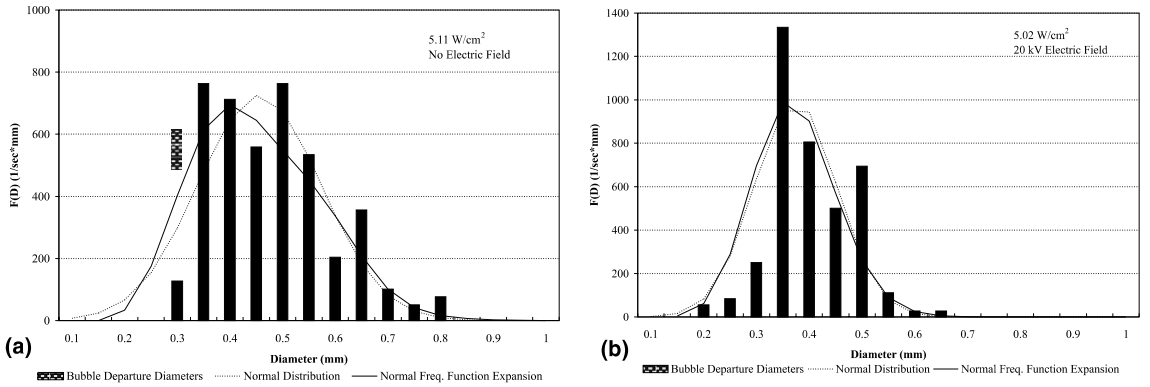

Fig. 3. (a) Bubble departure diameter distribution (no electric field). (b) Bubble departure diameter distribution (with electric field).

Table 1
Latent heat flux data

Total heat flux (W/cm^2)	5.11	5.02	7.85	7.88	11.33	11.06
Electrode voltage (kV)	0	20	0	20	0	20
Number of random samples	15	14	72	83	15	20
Number of bubbles measured	167	140	599	615	476	197
Number of nucleation sites	240	163	522	337	918	433
Heat transfer area (cm^2)	4.13	4.13	4.13	4.13	4.13	4.13
$\langle N \rangle$ (cm^{-2})	58.1	39.5	126.4	81.6	222.3	104.8
$\langle D \rangle$ (mm)	0.456	0.374	0.523	0.434	0.383	0.393
σ_D (mm)	0.117	0.078	0.127	0.102	0.074	0.083
Bubble departure period (s)	0.00471	0.00514	0.00391	0.00559	0.00423	0.00424
$\langle F \rangle$ (s^{-1})	212.3	194.6	255.8	178.9	236.4	235.8
ρ_v (kg/ m^3)	8.37	8.35	8.28	10.18	9.97	10.23
h_{fg} (kJ/kg)	167	167	167	165	165	165
$\langle J \rangle$ (J)	8.31×10^{-5}	4.33×10^{-5}	1.22×10^{-6}	8.38×10^{-5}	5.36×10^{-5}	6.07×10^{-5}
Latent heat flux, q'' (W/cm^2)	1.0	0.3	4.0	1.2	2.8	1.5

The heat flux due to latent heat transport, q'', was calculated using the following equation:

$$q'' = \langle N \rangle \langle J \rangle \langle F \rangle, \tag{1}$$

where $\langle J \rangle$ is the average heat removal per bubble (see [4]). Error propagation analysis showed that the estimated error in the value of $\langle J \rangle$ was 28.7%, with the largest contributor being the bias error in bubble departure diameter. As a result, the estimated error in the calculated latent heat flux contribution, q'', was 39%. Table 1 shows a comparison of the bubble statistics and latent heat contribution to the total heat flux between experiments at three different powers with and without an electric field. Table 2 shows the uncertainty data for the measured parameters. Application of an electric field resulted in fewer active nucleation sites and smaller bubble departure diameters; therefore, for a given heat flux, the latent heat contribution to the total heat flux with an applied electric field was smaller than without an electric field. As noted in [4], at a given heat flux, the suppression of boiling with an applied electric field is due to enhanced natural convection. The electric field causes mixing of the boundary layer preventing sufficient superheat to develop on the surface to support boiling. Therefore, an applied electric field increases the heat transfer coefficient, reduces the surface temperature, and delays the onset of boiling. According to Bergles [7], there are 14 enhancement techniques that are used to enhance pool boiling. The application of an electric field provides comparable results as these other techniques and can be used in conjunction with other enhancement techniques to produce a compound enhancement.

Table 2
Latent heat flux measured data uncertainty

	Uncertainty
Heater voltage	0.0002 (%)
Heater current	1 (%)
Heater width	0.025 (cm)
Heater length	0.025 (cm)
Number of nucleation sites	5 (%)
Measured bubble diameter	0.5 (mm)
Measured bubble period	0.0013 (s)

4. Conclusion

The purpose of this investigation was to demonstrate the use of a transparent ITO heater in studying bubble dynamics on flat heated surfaces and to quantify the effect of an electric field on bubble dynamics in saturated nucleate pool boiling. High speed video images were obtained for saturated pool boiling from a flat ITO surface immersed in R-123, with and without an applied uniform electric field. The use of a transparent heater allowed direct observation and recording of the bubble dynamics from underneath the heated surface. The bubble statistics including number of nucleation sites, bubble departure diameter, and bubble departure frequency were measured. For a given heat flux, application of an electric field reduces the surface temperature, thereby suppressing boiling and reducing the latent heat contribution to the total heat flux.

References

[1] G.E. Thorncroft, J.F. Klausner, R. Mei, Experimental investigation of bubble growth and detachment in vertical upflow and downflow boiling, Int. J. Heat Mass Transfer 41 (23) (1998) 3857–3871.

[2] N.R. Lynam, Transparent electronic conductors, Proc. Electrochem. Soc. 90 (2) (1990) 201–231.
[3] C.C. Pascual, Electrohydrodynamic enhancement of nucleate pool boiling, Ph.D. Thesis, Georgia Institute of Technology, Atlanta, GA, 1999.
[4] C.C. Pascual, S.M. Jeter, S.I. Abdel-Khalik, A statistical analysis of EHD-enhanced nucleate boiling along a heated wire, Int. J. Heat Mass Transfer 44 (2001) 1201–1212.
[5] D.D. Paul, S.I. Abdel-Khalik, A statistical analysis of saturated nucleate boiling along a heated wire, Int. J. Heat Mass Transfer 26 (1983) 509–519.
[6] R.S. Figliola, D.E. Beasley, Theory and Design for Mechanical Measurements, third ed., Wiley, New York, 2000.
[7] A.E. Bergles, Enhancement of pool boiling, Int. J. Refrig. 20 (8) (1997) 545–551.